European Review for Medical and Pharmacological Sciences 2023; 27: 11222-11235

Multi-targeted therapeutic effects of Sankudiwan (SKDW) in myocardial ischemia-reperfusion injury: a comprehensive study

Y. SUN[1], Q. JIA[2], L. LI[3], Y.-Q. TONG[4], D. ZOU[4], Y.-H. LIU[5], J.-Z. ZHANG[6]

[1]Baishan Hospital, Changchun University of Traditional Chinese Medicine, Baishan, Jilin, China
[2]Department of Laboratory, Affiliated Hospital of Changchun University of Traditional Chinese Medicine, Changchun, Jinlin, China
[3]Medical Insurance Office, Affiliated Hospital of Changchun University of Traditional Chinese Medicine, Changchun, Jinlin, China
[4]Department of Nephrology, Affiliated Hospital of Changchun University of Traditional Chinese Medicine, Changchun, Jinlin, China
[5]Department of Traditional Chinese Medicine Fundamentals, Changchun University of Traditional Chinese Medicine, Changchun, Jilin, China
[6]Affiliated Hospital, Changchun University of Traditional Chinese Medicine, Changchun, Jinlin, China

Abstract. – OBJECTIVE: This study aimed to investigate the therapeutic effects and underlying mechanisms of Sankudiwan (SKDW) on myocardial ischemia-reperfusion injury (MIRI) in a rat model.

MATERIALS AND METHODS: Rats were subjected to MIRI and treated with varying doses of SKDW. The myocardial infarct size, cardiac function, histological changes, apoptosis, and inflammation were assessed using TTC staining, echocardiography, Hematoxylin and Eosin (HE) staining, TUNEL staining, and ELISA assays. We further explored SKDW's influence on cardiomyocyte mitochondria and inflammatory factor expression. Moreover, oxidative stress-related parameters and differentially expressed genes were analyzed using bioinformatics approaches.

RESULTS: SKDW significantly reduced myocardial infarct size and improved cardiac function, demonstrating a dose-dependent therapeutic potential. It ameliorated myocardial tissue damage at the histological level, inhibited cardiomyocyte apoptosis, and mitigated inflammatory response. SKDW also enhanced mitochondrial energy metabolism and suppressed the levels of oxidative stress markers. Bioinformatics analysis identified key differentially expressed genes (DEGs), including cbln1, Tgm1, Trh, and Ccl27, possibly mediating the therapeutic effects of SKDW.

CONCLUSIONS: SKDW exerts its therapeutic effects on MIRI through the modulation of several genes and pathways related to inflammation, apoptosis, mitochondrial function, and oxidative stress. Our findings provide a scientific basis for the clinical application of SKDW in the treatment of MIRI.

Key Words:
Sankudiwan, Myocardial ischemia-reperfusion injury, Inflammation, Oxidative stress, Apoptosis, Bioinformatics.

Introduction

Myocardial Ischemia-Reperfusion Injury (MIRI) remains a significant cause of morbidity and mortality in cardiovascular diseases across the globe, affecting millions of people each year[1]. Despite the improvement in early revascularization strategies, MIRI continues to pose substantial challenges, primarily due to the paradoxical exacerbation of myocardial injury following reperfusion, a process often referred to as "reperfusion injury"[2].

Clinical management of MIRI predominantly involves interventions aimed at restoring coronary blood flow and minimizing myocardial damage. However, the phenomenon of "reperfusion injury" renders this a double-edged sword, leading to further myocardial damage even after successful revascularization[3]. Additionally, the current pharmacological treatments have yielded only modest reductions in infarct size and improvements in long-term clinical outcomes, revealing a substantial therapeutic gap in managing MIRI.

The use of traditional Chinese medicine (TCM) in the treatment of myocardial ischemia-reperfusion injury (MIRI) has gained significant attention due to its potential in alleviating cardiac

Corresponding Author: Jingzhou Zhang, MD; e-mail: zjz362@126.com

injury and restoring heart function[4]. Multiple components found in TCM, such as saponins, flavonoids, and alkaloids, have demonstrated beneficial effects in reducing inflammation, oxidative stress, and cardiomyocyte apoptosis, key pathological processes in MIRI[5]. Despite these promising findings, the use of TCM in MIRI treatment is not without limitations. Many studies lack rigorous design and robust analysis, resulting in the potential for bias and confounding factors[6]. Furthermore, the specific mechanisms underlying the therapeutic effects of TCM in MIRI are not fully understood, mainly due to the complex nature of TCM compounds and the intricate interplay between different signaling pathways in MIRI. Therefore, more high-quality studies are warranted to explore the potential benefits and underlying mechanisms of TCM in MIRI treatment.

Sankudiwan (SKDW), an intriguing focus of our study, is a traditional Chinese herbal formulation comprised of two central medicinal herbs, Sanqi and *Crepidiastrum sonchifolium*. Sanqi, also known as *Panax notoginseng*, is a traditional Chinese herb that has been used for centuries in traditional Chinese medicine. It is known for its various pharmacological effects and health benefits. One of the key benefits of Sanqi is its ability to promote blood circulation and relieve blood stasis. It has been traditionally used to treat various conditions related to poor blood circulation, such as bruises, bleeding, and cardiovascular diseases[7]. Sanqi contains active compounds called saponins, which have been found to have anti-inflammatory, antioxidant, and antithrombotic properties[8]. These properties contribute to its ability to improve blood flow and prevent the formation of blood clots[8]. Crepidiastrum sonchifolium is an annual forb plant native to East Asia, including China and Korea. It belongs to the Asteraceae family and is known for its various uses in traditional medicine and culinary applications[9]. It is extensively used in herbal medicines in East Asia, particularly for treating conditions such as inflammation, blood circulation disorders, and eye-related diseases[9]. The combination of these herbs in SKDW enhances their therapeutic potential, synergistically promoting blood circulation, resolving stasis, and alleviating pain. The prospect of SKDW's therapeutic effects against MIRI motivates the investigation of its potential and the mechanisms at play in this study.

In light of the prevailing challenges in MIRI treatment and the potential therapeutic promise of SKDW, we embarked on this study to investigate the therapeutic potential and mechanisms of action of SKDW in MIRI. We aim to enhance our understanding of the pathophysiology of MIRI and contribute towards the development of more effective therapeutic strategies.

Materials and Methods

Ethic Statement and Grouping

Seventy specific-pathogen-free (SPF) SD rats (6-7 weeks old, weighing 200-220 g) were adaptively raised for 7 days. These rats were randomly divided into five groups: Control, Sham, Sanku Dropping Pill (high, medium, low dosage), and a positive control group [Danshen dropping pills, (DSDP)], each group consisting of 10 rats. After 7 days of consecutive gavage, the rat myocardial ischemia-reperfusion injury (MIRI) model was constructed (ischemia for 30 minutes, reperfusion for 2 hours).

(1) Control group: no interventions were carried out on the rats in this group.

(2) Sham group: rats were administered an equivalent volume of 0.5% sodium carboxymethyl cellulose solution for 7 days, after which surgical modeling was conducted without occlusion of blood flow.

(3) MIRI group: rats were administered an equivalent volume of 0.5% sodium carboxymethyl cellulose solution for 7 days, after which ischemia was induced for 30 minutes, followed by reperfusion for 2 hours.

(4) San Kudri Myrobalan group: rats in the low, medium, and high dosage groups were daily gavaged with San Kudri Myrobalan at 0.8 (20 times the normal adult dosage), 1.6 (40 times the normal adult dosage), and 3.2 g/kg (80 times the normal adult dosage), respectively. The modeling was conducted after the final dose administration.

(5) Positive control group (Danshen dropping pills): rats were daily gavaged with Danshen dropping pills at 0.4 g/kg for 7 days. The modeling was conducted after the final dose administration.

After the completion of modeling, fecal tissue samples were collected from each group and stored at -80°C. After ultrasonically assessing cardiac functions, serum and myocardial tissue were collected from each rat. Half of the myocardial tissue was fixed in 4% paraformaldehyde, and the other half was stored at -80°C.

All experimental procedures were performed in accordance with the ARRIVE guidelines (www.nc3rs.org.uk/ARRIVE) and the National

Institutes of Health Guide for the Care and Use of Laboratory Animals (NIH Publication No. 85-23, revised 1996). This study was approved by the Ethics Committee of our institution (Approval No. 2021442).

Establishment of Myocardial Ischemia-Reperfusion Injury Rat Model

The myocardial ischemia-reperfusion injury (MIRI) model was established using a method adapted from the literature[10]. After anesthetizing the rats with 2% pentobarbital sodium (50 mg/kg) injected intraperitoneally, they were placed in the supine position on a heated pad to maintain a body temperature of 37°C. A tracheal intubation was performed for ventilation with a small animal respirator, setting the tidal volume at 10 ml/kg and maintaining the respiratory rate at 70 breaths per minute. Subsequently, a left thoracotomy was carried out at the fourth intercostal space to expose the heart, followed by identifying and ligating the left anterior descending coronary artery (LAD) with a 6-0 silk suture. The left ventricle's anterior wall discoloration confirmed occlusion. For the ischemia phase, the LAD was ligated for 30 minutes, then the ligature around the LAD was released allowing for reperfusion, which was confirmed by the return of color to the anterior wall of the left ventricle and lasted for 2 hours. For the Sham group, the procedure was carried out identically, but without ligating the LAD, therefore not interrupting the blood flow. At the end of the experiment, rats were euthanized under deep anesthesia and tissues were harvested for further analysis. The entire procedure was performed with aseptic precautions.

Triphenyl Tetrazolium Chloride (TTC) Staining

Sprague-Dawley rats were anesthetized, and their hearts were extracted, flash-frozen at -20°C for 20 minutes, and then sectioned into 5-6 slices (2 mm thick each). The slices were incubated in 2% TTC solution, covered, and heated at 37°C for 15-30 minutes. Post incubation, images were captured for myocardial infarction area analysis using Image-Pro Plus 6.0 software.

Echocardiographic Assessment of Rat Hearts

For this procedure, one rat was randomly selected from each group. The selected rats were anesthetized and secured in a supine position. Hair from the left anterior chest area was removed using a 10% sodium sulfide solution to ensure optimal imaging quality. A blinded operator performed echocardiographic evaluations of the left ventricular function. Measurements taken included: left ventricular end-diastolic diameter (LVEDd), left ventricular end-systolic diameter (LVESd), end-diastolic left ventricular volume (LVEDV), end-systolic left ventricular volume (LVESV), left ventricular ejection fraction (LVEF), and left ventricular fractional shortening (LVFS). These parameters provide a comprehensive assessment of the functional status of the left ventricle.

TUNEL and Hematoxylin and Eosin (HE) Staining of Rat Heart Tissue

To conduct the histopathological analysis, hearts were extracted, and the ventricular chamber was rinsed with saline. The external morphology of the hearts was observed visually. Ventricular samples were then excised and fixed in 4% polyformaldehyde. Post-fixation, tissues underwent dehydration and were subsequently embedded in paraffin. The paraffin-embedded tissue samples were then sectioned. Hematoxylin and Eosin (HE) staining was performed on the sections to analyze the infiltration of inflammatory cells. This process ensured comprehensive histological examination and enabled the identification of changes in the heart tissue due to the disease and subsequent treatment.

Transmission Electron Microscopy Analysis of Cardiomyocyte Mitochondria

For each group, one rat was randomly selected. The rats were anesthetized, and the hearts were swiftly removed and immersed in 2.5% glutaraldehyde solution (Sigma-Aldrich, St. Louis, MO, USA) at 4°C for 24 hours for primary fixation. Tissue samples from the left ventricle were then excised, approximately 1 mm in size, and kept in the same fixative at 4°C until further processing. Post-fixation was performed in 1% osmium tetroxide (OsO_4; Sigma-Aldrich, St. Louis, MO, USA) for 2 hours at room temperature, followed by a series of dehydration steps in graded ethanol concentrations (50%, 70%, 90%, and 100%) and propylene oxide. The samples were then embedded in Epon 812 resin (Sigma-Aldrich, St. Louis, MO, USA) and polymerized at 60°C for 48 hours. Ultrathin sections (70 nm) were cut using an ultramicrotome (Leica Microsystems, Wetzlar, Germany) and collected on 200 mesh copper grids. The grids were stained with uranyl acetate and

lead citrate (Sigma-Aldrich, St. Louis, MO, USA) to enhance the contrast. Images of the mitochondria were captured using a transmission electron microscope (Hitachi, Tokyo, Japan) to study their morphology, division, and aggregation. Special attention was paid to any observable alterations in the cardiomyocyte autophagy status. Image acquisition and analysis were performed by a researcher blinded to the experimental groups.

Enzyme-Linked Immunosorbent Assay (ELISA)

In our study, serum and myocardial tissue biomarkers were analyzed using ELISA kits. Serum biomarkers including cardiac troponin I (cTnI), interleukins (IL-6, IL-10, IL-13, and IL-4), tumor necrosis factor-alpha (TNF-α), creatine kinase (CK), aspartate aminotransferase (AST), lactate dehydrogenase (LDH), nitric oxide (NO), malondialdehyde (MDA), superoxide dismutase (SOD), and myeloperoxidase (MPO) were assessed using specific ELISA kits, following the manufacturer's instructions. Similarly, myocardial tissue biomarkers, including NO, MDA, SOD, MPO, and CK, were also quantified using specific ELISA kits. All the assays were conducted strictly adhering to the protocols provided with the respective kits (Nanjingjiancheng, China). To ensure the accuracy of the results, all samples were analyzed in triplicate. The absorbance was measured at the specified wavelength using a microplate reader, and the concentration of each biomarker was calculated from the standard curve generated for each assay.

Quantitative Reverse Transcription Polymerase Chain Reaction (RT-qPCR)

The expression levels of specific genes (TNF-α, IL-4, IL-6, IL-10, and IL-13) in myocardial tissue were measured using RT-qPCR. The total RNA was extracted from the tissue samples using the RNeasy Mini Kit (Qiagen, Germany). Complementary DNA (cDNA) was synthesized from the total RNA using the High-Capacity cDNA Reverse Transcription Kit (Applied Biosystems, USA). Subsequently, qPCR was conducted using the PowerUp SYBR Green Master Mix (Applied Biosystems, USA) on a StepOnePlus Real-Time PCR System (Applied Biosystems, USA). The primer sequences for TNF-α, IL-4, IL-6, IL-13, and GAPDH were designed and synthesized by Integrated DNA Technologies (USA). Each reaction was performed in triplicate, and the results were analyzed using the 2^-ΔΔCT method.

Transcriptomic Analysis and Pathway Enrichment

In this research, we utilized transcriptome sequencing to analyze gene expression alterations in rat myocardial tissue samples post-SKDW treatment for MIRI. We extracted total RNA from the samples *via* the TRIzol Reagent (Invitrogen, USA) and evaluated its integrity using the Bioanalyzer 2100 system (Agilent Technologies, USA). Using the NEBNext Ultra RNA Library Prep Kit (New England Biolabs, USA), we prepared libraries following the manufacturer's protocol, and performed sequencing on an Illumina Novaseq platform (Illumina, USA). The raw reads generated were cleaned and mapped to the rat reference genome (Rnor_6.0) using Hisat2. We then conducted GSEA to identify significantly enriched pathways in DEGs using the KEGG database, with all bioinformatics analyses performed using R (version 3.6.3) and Bioconductor, and a false discovery rate (FDR) controlled by the Benjamini and Hochberg's approach. An adjusted p-value of < 0.05 was deemed statistically significant.

Statistical Analysis

All statistical analyses were conducted using IBM SPSS Statistics software (International Business Machines Corp., Armonk, NY, USA) and GraphPad Prism (GraphPad Software, Inc., La Jolla, CA, USA). Data are represented as mean ± standard deviation (SD) of three independent replicate experiments. Significance was determined by one-way analysis of variance (ANOVA) followed by the Student's t-test. Statistical significance was set at $*p < 0.05$, $**p < 0.01$, $***p < 0.001$, in comparison with the control group.

Results

Evaluation of SKDW's Therapeutic Impact on Myocardial Ischemia-Reperfusion Injury (MIRI)

To evaluate the therapeutic effect of SKDW on MIRI, we administered three different doses of SKDW (high, medium, and low), with the clinically recognized effective treatment, DSDP, serving as the positive control. TTC staining results indicated no myocardial infarction in the control group, minimal infarction in the Sham group, while the most extensive myocardial infarction was observed in the Model group. SKDW significantly reduced the infarct size in a dose-dependent manner. The high-dose SKDW (SKDW-H)

treatment demonstrated the most efficacy, comparable to the DSDP group (Figure 1A, C). Echocardiogram results showed a significant decrease in fractional shortening (FS) and ejection fraction (EF) in the model group compared to both the control and sham groups. However, SKDW administration displayed a dose-dependent recovery of cardiac function, with no significant difference noted between the high-dose SKDW (SKDW-H) and DSDP groups (Figure 1B, D, E). Furthermore, in comparison to the Control and Sham groups, cardiac troponin I (cTnI) was significantly upregulated in the Model group. Meanwhile, SKDW showed a dose-dependent reduction in its expression (Figure 1F). These results suggest that SKDW exhibits therapeutic potential for MIRI, with the high-dose SKDW (SKDW-H) showing the greatest effectiveness.

HE Staining Assessment of the Therapeutic Effect of SKDW on Infarcted Myocardial Tissue

To further elucidate the therapeutic efficacy of SKDW, histological changes in the infarcted myocardial tissue were observed using Hematoxylin and Eosin (HE) staining. In the Control and Sham groups, rat myocardial tissues exhibited well-arranged muscle fibers and evenly distributed cell

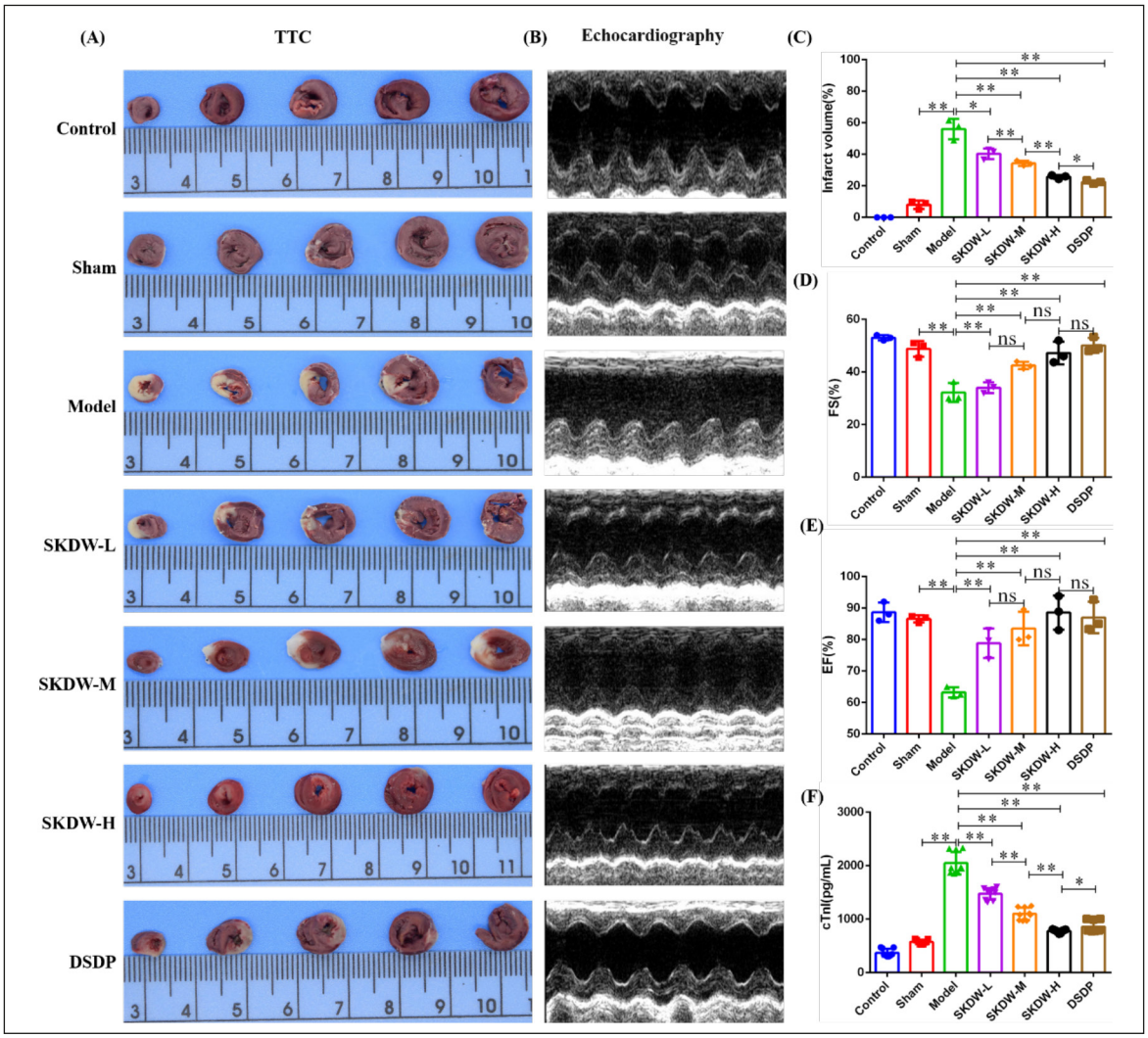

Figure 1. Evaluation of Sankudiwan (SKDW) therapeutic impact on myocardial ischemia-reperfusion injury (MIRI). **A**, TTC-stained myocardial tissues from seven experimental groups: control, sham, model, low-dose SKDW (SKDW-L), medium-dose SKDW (SKDW-M), high-dose SKDW (SKDW-H), and positive control (DSDP). **B**, Echocardiogram images displaying the cardiac function of the different groups. **C**, Quantitative analysis of the infarct size area. **D**, Fractional shortening (FS) and (**E**) Ejection fraction (EF) data obtained from the echocardiography. **F**, Cardiac troponin I (cTnI) expression levels determined by ELISA. ns: not significant, $*p < 0.05$, and $**p < 0.01$.

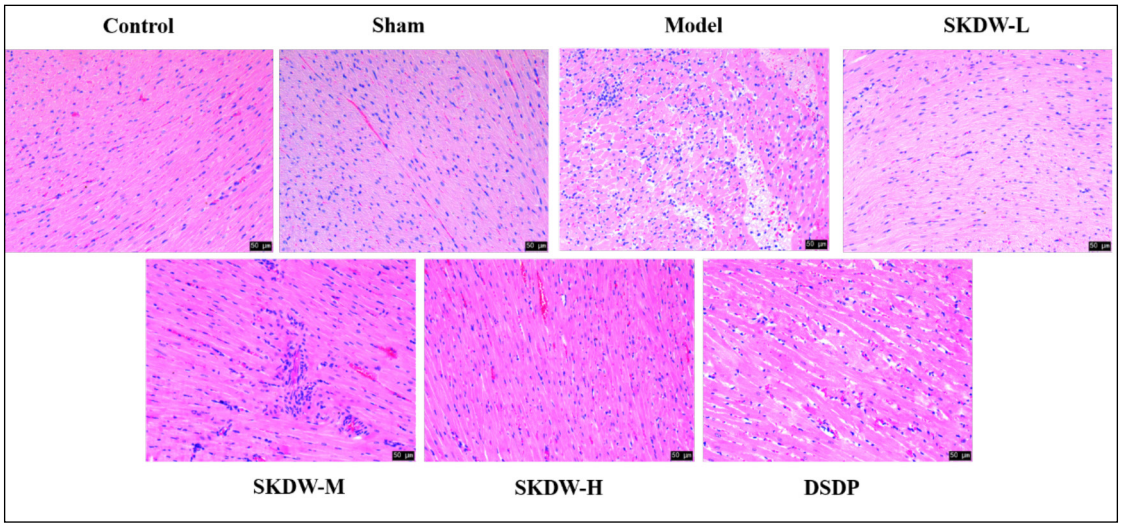

Figure 2. Hematoxylin and Eosin (HE) staining assessment of the therapeutic effect of SKDW on infarcted myocardial tissue. HE-stained myocardial tissues from seven experimental groups: control, sham, model, low-dose SKDW (SKDW-L), medium-dose SKDW (SKDW-M), high-dose SKDW (SKDW-H), and positive control (DSDP).

nuclei. Conversely, the model group showed disorganized muscle fiber arrangement and an abundance of clustered cell nuclei. Post-SKDW treatment, a marked improvement was seen in muscle fiber arrangement, and a reduction in nuclear clustering was observed. Notably, myocardial tissue from the high-dose SKDW (SKDW-H) group bore a resemblance to that of the DSDP group. These results confirm that SKDW can ameliorate myocardial tissue damage at the histological level (Figure 2).

Assessment of SKDW's Influence on Cardiomyocyte Apoptosis Using TUNEL Staining

Further, we employed TUNEL staining to evaluate the impact of SKDW on cardiomyocyte apoptosis. The findings revealed that nearly no TUNEL-positive cells were detectable in the control and sham groups, signifying minimal apoptosis. However, the model group exhibited a significant number of apoptotic cells. Compared to the model group, SKDW treatment resulted in a dose-dependent reduction in the quantity of apoptotic cells. Importantly, no statistically significant difference was noted in the number of apoptotic cells between the high-dose SKDW (SKDW-H) group and the DSDP group. These results suggest that SKDW can dose-dependently inhibit cardiomyocyte apoptosis (Figure 3).

Exploring the Therapeutic Mechanism of SKDW on Cardiomyocyte Mitochondria

To understand the therapeutic mechanisms of SKDW, we further evaluated its influence on cardiomyocyte mitochondria. In the Control and Sham groups, cardiomyocyte mitochondria exhibited fusiform and round shapes, with clearly discernible cristae structures. However, in the Model group, the mitochondria appeared shrunken or swollen, with obscured mitochondrial membrane clarity. Upon treatment with SKDW, improvements in mitochondrial morphology were evident, with the most pronounced effects observed in the SKDW-H group (Figure 4). These findings suggest that the therapeutic effects of SKDW could potentially be attributed to its influence on mitochondrial energy metabolism in cardiomyocytes.

Evaluation of the Therapeutic Effects of SKDW on Inflammatory Factor Expression

To further evaluate the therapeutic effects of SKDW, we used ELISA and RT-qPCR to measure the expression levels of several inflammatory factors in the blood and myocardial tissues. In the control and sham groups, the expression levels of TNF-α, IL-4, IL-6, and IL-13 were relatively low in both the rat serum and myocardial tissues. However, their expression levels markedly in-

creased in the model group. Interestingly, the administration of SKDW demonstrated a dose-dependent reduction in these inflammatory factors compared to the model group. On the contrary, the expression of IL-10 was comparatively high in the control and sham groups but significantly decreased in the model group. This downward trend was effectively countered by a dose-dependent increase in IL-10 expression with SKDW treatment. These results suggest that SKDW can significantly suppress the levels of inflammatory factors in both myocardial tissues and blood (Figure 5), further confirming its therapeutic potential.

Assessment of the Effect of SKDW on Oxidative Stress

Oxidative stress plays a pivotal role in the molecular mechanism of myocardial ischemia-reperfusion injury (MIRI). Consequently, we evaluated several oxidative stress-related parameters in the blood serum and myocardial tissues. In the serum of the control and sham groups, the levels of NO, MDA, MPO, FG, LDH, and AST were relatively low, while the SOD level was high. Conversely, the model group exhibited a substantial increase in the levels of NO, MDA, MPO, FG, LDH, and AST, alongside a significant reduction in SOD. The administration of SKDW led to a dose-dependent inhibition of NO, MDA, MPO, FG, LDH, and AST levels, while simultaneously enhancing SOD levels. Similarly, in the myocardial tissues, the control and sham groups presented with low expression levels of NO, MDA, MPO, and CK and higher expression levels of SOD. However, the model group showed a pronounced increase in the expression of NO, MDA, MPO, and CK. SKDW, in a dose-dependent manner, suppressed the expression of NO, MDA, MPO, and CK in myocardial tissue, while enhancing SOD expression (Figure 6). These results suggest that SKDW could mitigate the oxidative stress condition in both myocardial tissues and systemically, reinforcing its therapeutic potential.

Identification of Key Differentially Expressed Genes Mediating the Therapeutic Effects of SKDW on MIRI

To further delineate the molecular mechanism underlying the treatment of myocardial ischemia-reperfusion injury (MIRI) by SKDW, we performed RNA sequencing to detect differential gene expressions among the groups. Our data revealed that 1,927 genes were upregulated and 2,713 genes were downregulated in the model group compared to the Sham group. When compared to the Model group, the SKDW-L group showed an upregulation of 1,267 genes and a downregulation of 2,713 genes. The SKDW-M group exhibited an upregulation of 1,369 genes and a downregulation of 2,351 genes. Intriguingly, the SKDW-H group only showed an upregulation of 167 genes and a downregulation of 195 genes compared to the model group (Figure 7).

Gene Ontology (GO) analysis indicated that the upregulated genes in the model group compared to the sham group were primarily associated with

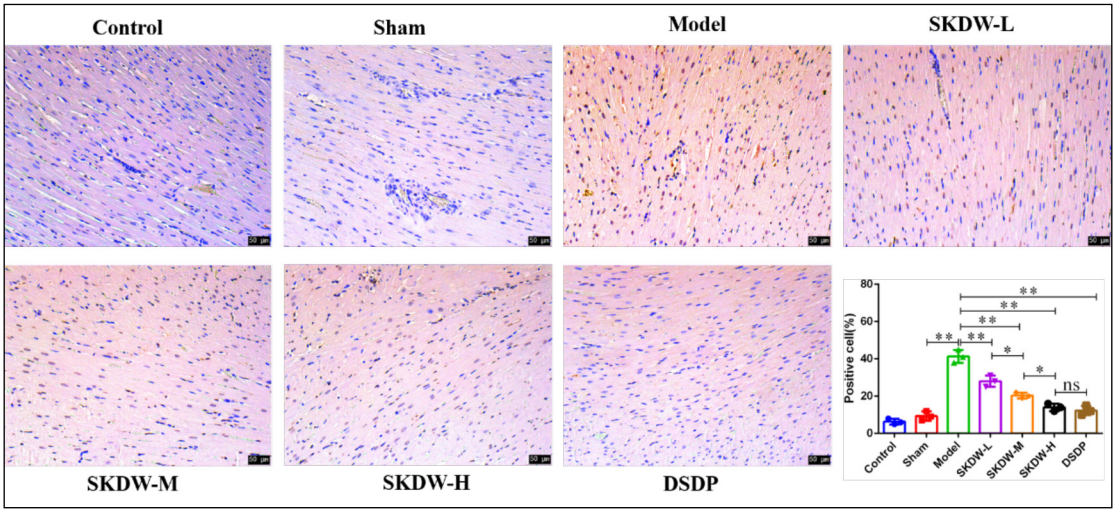

Figure 3. TUNEL staining assessment of the therapeutic effect of SKDW on infarcted myocardial tissue. TUNEL stained myocardial tissues from seven experimental groups: Control, Sham, Model, low-dose SKDW (SKDW-L), medium-dose SKDW (SKDW-M), high-dose SKDW (SKDW-H), and positive control (DSDP). ns: not significant, $*p < 0.05$, and $**p < 0.01$.

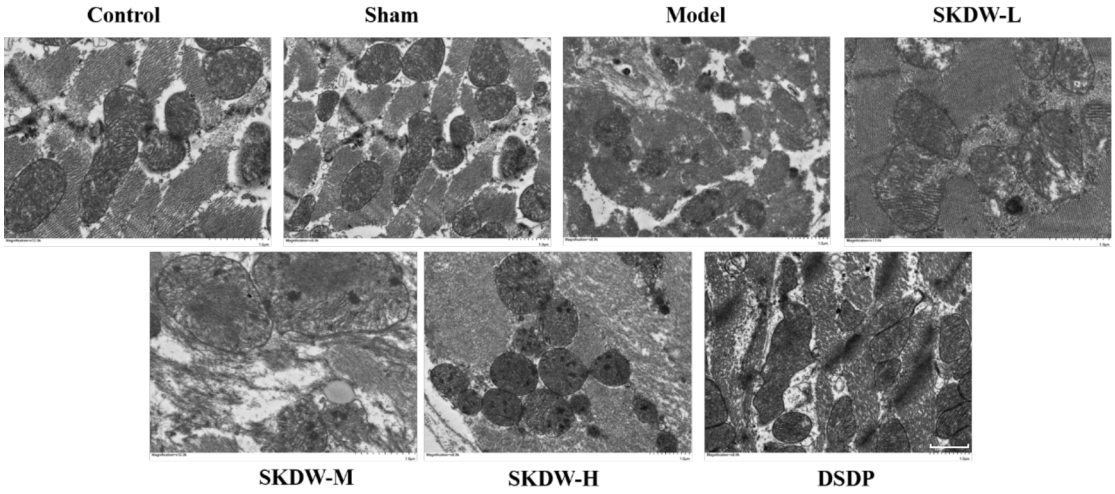

Figure 4. Exploring the therapeutic mechanism of SKDW on cardiomyocyte mitochondria.

oxidoreductase activity and catalytic activity. In contrast, downregulated genes were mainly involved in signal transduction and immune response. The downregulated genes in the SKDW-H group compared to the model group were mostly involved in immune response and extracellular region, while upregulated genes were predominantly associated with plasma membrane and homophilic cell adhesion *via* plasma membrane (Figure 8).

KEGG pathway analysis showed that upregulated genes in the model group compared to the sham group were mainly implicated in the biosynthesis of secondary metabolites, thermogenesis, oxidative phosphorylation, and microbial metabolism in diverse environments. On the other hand, downregulated genes were primarily involved in cytokine-cytokine receptor interaction, phagosome, and chemokine signaling pathways. In the SKDW-H group compared to the model group, the downregulated genes were primarily involved in cytokine-cytokine receptor interaction, while upregulated genes were mostly associated with hematopoietic cell lineage, peroxisome, and chemokine signaling pathway (Figure 9).

We speculated that SKDW may exert its effects by modulating the expression of certain genes. Therefore, we utilized Venn diagrams to identify shared differentially expressed genes among the different groups. Specifically, we intersected upregulated/downregulated gene sets from model/sham with the downregulated/upregulated gene sets from SKDW/Model to pinpoint key genes involved in the therapeutic effects of SKDW. Our results demonstrated that the gene cbln1 was a shared gene among the downregulated gene sets in the SKDW-H/Model and SKDW-M/Model and the upregulated gene set in model/sham. Similarly, Tgm1, Trh, and Ccl27 were shared genes among the upregulated gene sets in the SKDW-H/Model and SKDW-M/Model and the downregulated gene set in Model/Sham (Figure 10). Hence, we posit that SKDW may exert its therapeutic effects by modulating the expression of cbln1, Tgm1, Trh, and Ccl27.

Discussion

Our findings underscore the dose-dependent therapeutic impact of SKDW on MIRI. This is marked by reduced myocardial infarction, enhanced cardiac function, and minimized myocardial tissue damage and cardiomyocyte apoptosis. Specifically, SKDW significantly diminished infarct size, displayed a dose-dependent recovery of cardiac function, and led to a dose-dependent reduction in cTnI, a marker of cardiac injury. Furthermore, SKDW treatment induced notable improvements in myocardial tissue arrangement and reduced nuclear clustering, along with a substantial decrease in cardiomyocyte apoptosis. Additionally, through bioinformatics analysis, our study unraveled differential gene expressions that may mediate the therapeutic effects of SKDW on MIRI. Importantly, cbln1, Tgm1, Trh, and Ccl27 were identified as potential key genes, suggesting that the therapeutic effects of SKDW might be

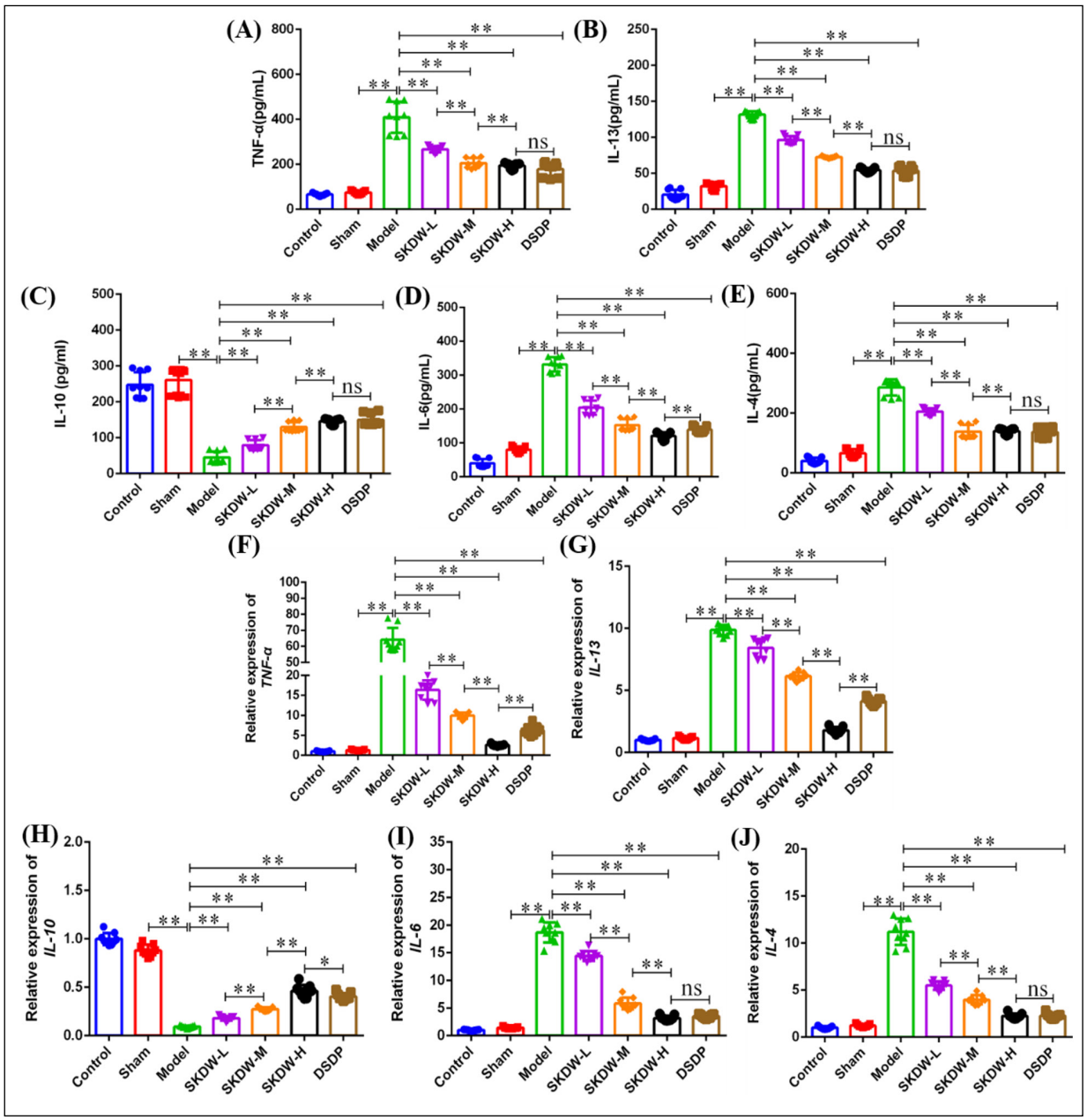

Figure 5. Evaluation of the therapeutic effects of SKDW on inflammatory factor expression. **A-E**, ELISA analysis of serum levels of inflammatory factors including TNF-α, IL-13, IL-10, IL-6, and IL-4, respectively, shown by the histogram, from Control, Sham, Model, SKDW-L, SKDW-M, SKDW-H, and DSDP groups. **F-J**, RT-qPCR analysis of the expression levels of TNF-α, IL-13, IL-10, IL-6, and IL-4 in the myocardial tissues represented by the histogram. ns: not significant, $*p < 0.05$, and $**p < 0.01$.

achieved by modulating the expression of these genes. These results offer further insights into the underlying molecular mechanism of SKDW's therapeutic potential in the context of MIRI. Taken together, these results validate the potential therapeutic benefits of SKDW against MIRI, particularly in its high-dose form.

Inhibiting cardiomyocyte apoptosis is of paramount importance in mitigating myocardial ischemia-reperfusion injury (MIRI), as apoptosis is a principal form of cell death in MIRI, leading to loss of functional myocardium and eventually heart failure[11]. Several key pathways have been identified as contributing factors to cardio-

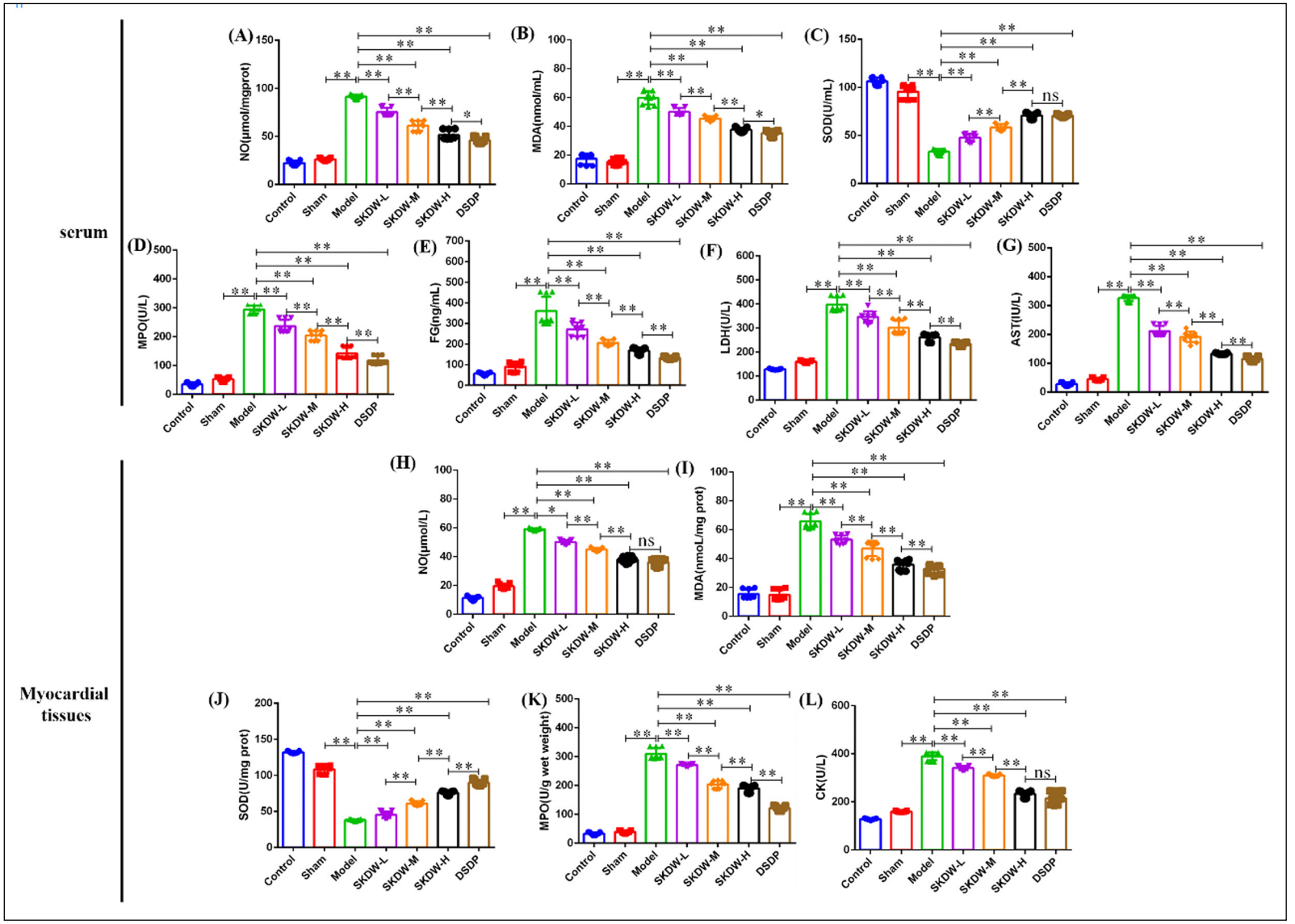

Figure 6. Assessment of the effect of SKDW on oxidative stress. **A-G**, ELISA analysis of serum levels of oxidative indicators including NO, MDA, MPO, SOD, FG, LDH, and AST, respectively, shown by the histogram, from Control, Sham, Model, SKDW-L, SKDW-M, SKDW-H, and DSDP groups. **H-L**, ELISA analysis of the expression levels of NO, MDA, MPO, SOD and CK in the myocardial tissues, represented by the histogram. ns: not significant, $*p < 0.05$, and $**p < 0.01$.

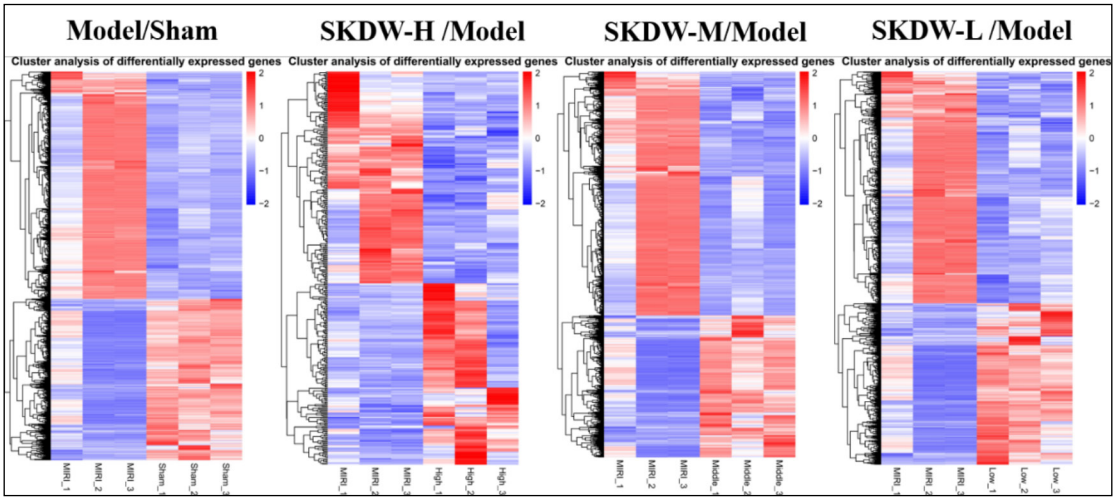

Figure 7. DEGs analyzed by heat map.

myocyte apoptosis in MIRI, including the intrinsic mitochondrial pathway, extrinsic death receptor pathway, and endoplasmic reticulum stress pathway[12]. These pathways, often activated by oxidative stress and inflammation, disrupt cellular homeostasis, leading to cardiomyocyte apoptosis[13]. In comparison to existing literature that primarily focuses on individual targets or pathways, our research provides a comprehensive investigation into the multi-targeted therapeutic effects of Sankudiwan (SKDW). Our findings show that SKDW not only reduces myocardial tissue damage and cardiomyocyte apoptosis but also improves cardiomyocyte mitochondrial morphology, furthering our understanding of the compound's efficacy against MIRI. These results highlight the potential of SKDW as a promising therapeutic agent for MIRI, warranting further clinical exploration.

Oxidative stress and inflammatory response play pivotal roles in the pathogenesis of myocardial ischemia-reperfusion injury (MIRI), leading to the initiation of cardiomyocyte apoptosis and consequent loss of myocardial tissue[14]. Many traditional Chinese medicines, such as *Salvia miltiorrhiza*, *Panax notoginseng*, and *Astragalus membranaceus*, have been demonstrated to exert protective effects against MIRI, mainly through their antioxidant, anti-apoptotic, and anti-inflammatory properties[15]. However, compared to these studies[14,15] focusing on single herbs, our investigation delves into the multi-faceted effects of Sankudiwan (SKDW), an herbal compound. Our results elucidate that SKDW not only attenuates myocardial tissue damage and cardiomyocyte apoptosis but also improves the morphology of cardiomyocyte mitochondria. This highlights the potential of SKDW as a promising therapeutic strategy for MIRI.

Our RNA sequencing results, in conjunction with GO and KEGG pathway analyses, have revealed several key genes – cbln1, Tgm1, Trh, and Ccl27 – that may underpin the therapeutic effect of SKDW on MIRI. Cbln1, primarily expressed in the cerebellum, plays an integral role in synapse integrity and function and has been associated with cardiac function, implying its potential involvement in cardioprotection[16]. Tgm1 is involved in processes such as inflammation, fibrosis, and wound healing, suggesting that its upregulation by SKDW might contribute to the repair and regeneration of myocardial tissue following ischemia-reperfusion injury[17]. Thyrotropin-releasing hormone (Trh) has been reported to exert cardioprotective effects, potentially by inhibiting apoptosis, enhancing myocardial contractility, and ameliorating reperfusion injury[18]. Ccl27, which regulates inflammation and immune response, could be instrumental in SKDW's anti-inflammatory action[19]. These findings add new dimensions to our understanding of SKDW's therapeutic mechanism in MIRI, warranting further exploration.

Limitations

Despite the promising results, this study does have certain limitations. First, it was conducted exclusively in a rat model, which may not entirely mimic the human condition, considering interspecies differences. Additionally, our study lacks longitudinal data to assess the long-term

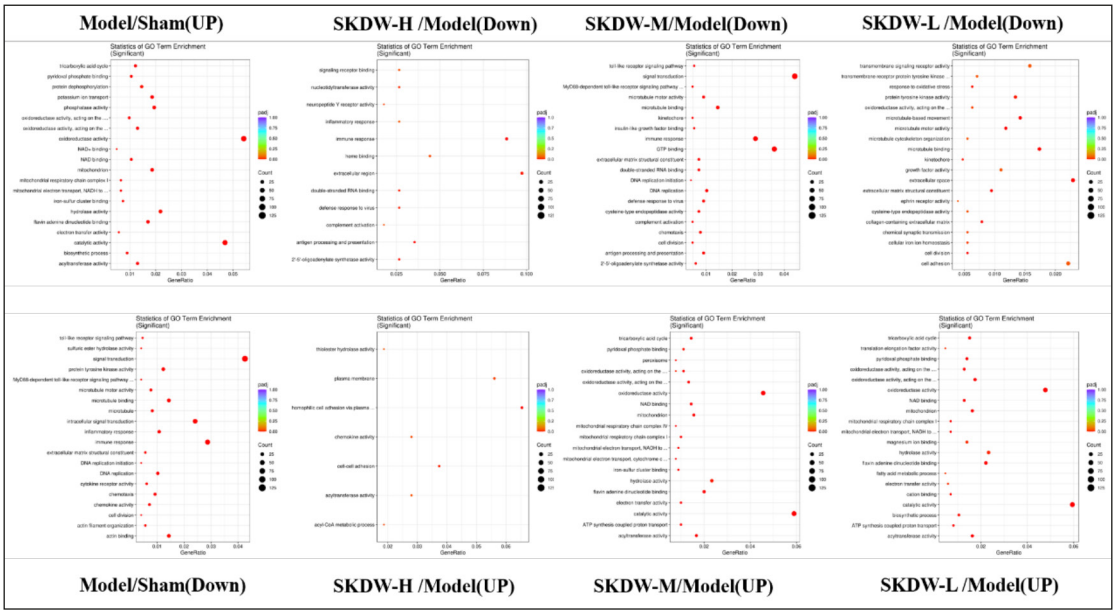

Figure 8. GO analysis of DEGs from different groups.

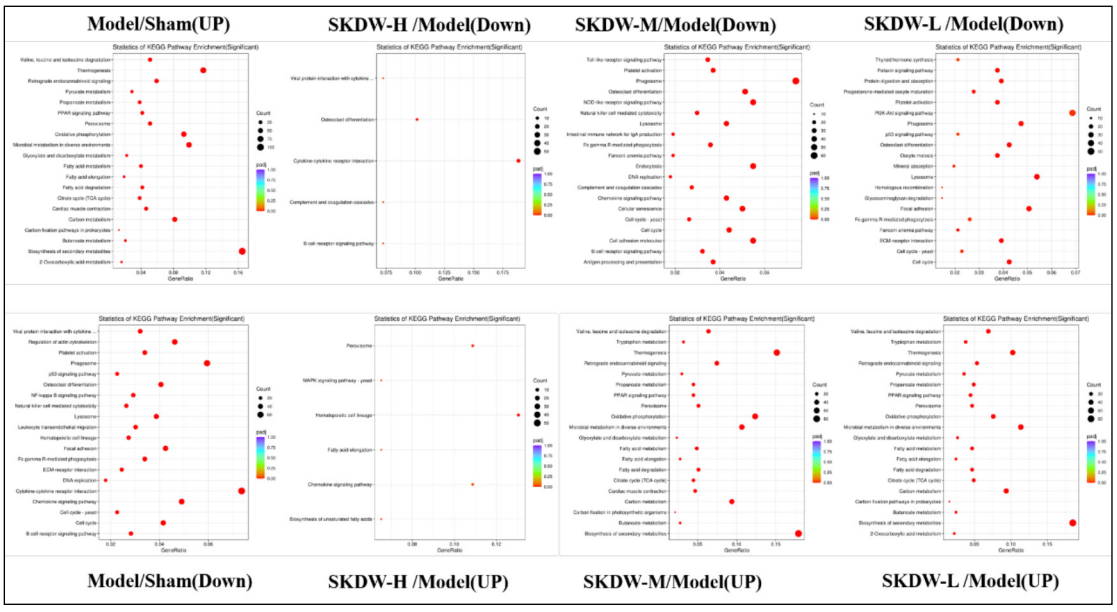

Figure 9. KEGG analysis of DEGs from different groups.

effect and safety of SKDW treatment. Furthermore, the specific molecular mechanisms through which SKDW exerts its therapeutic effects remain unclear and warrant more comprehensive investigation. For future research, we recommend validating these preliminary findings in larger, multicentric trials, and potentially in different animal models. Translating these findings into clinical practice will also require rigorous clinical trials to assess the safety, tolerability, and efficacy of SKDW in patients with myocardial infarction.

Conclusions

Our study suggests that SKDW alleviates MIRI in rats by modulating several key biological processes and pathways, shedding new

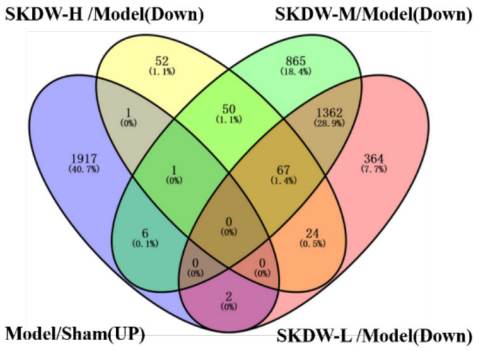

Gene	log2FoldChange			
	Model/Sham	SKDW-H /Model	SKDW-M /Model	SKDW-L/Model
Myo16	1.7759	-2.4697		
Cbln1	2.152	-1.9656	-2.7273	
Ptprt	2.3972		-1.6513	
RGD1305184	1.6285		-3.4774	
LOC100911030	1.0223		-2.7176	
Chac1	2.0905		-1.7831	
RT1-N2	1.8959		-1.151	
Nalcn	1.7923		-1.7314	
Adh1	2.1629			-1.6874
Myl7	3.0309			-2.5678

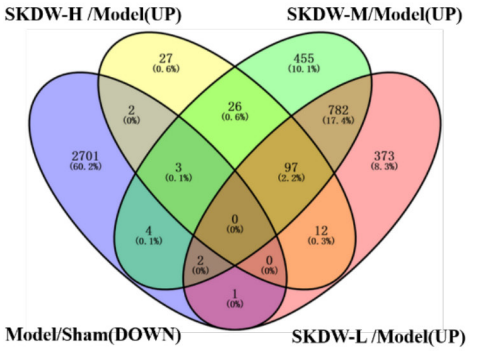

Gene	log2FoldChange			
	Model/Sham	SKDW-H /Model	SKDW-M /Model	SKDW-L/Model
Ccl9	-2.0148	2.2294		
Dsc3	-5.7252	2.0551		
Tgm1	-2.3724	3.0041	3.3985	
Trh	-1.6196	1.994	1.8803	
Ccl27	-1.2679	1.7703	2.0407	
Lcn2	-3.5479		1.812	
Mt1m	-2.2114		2.6076	
Fhad1	-2.7108		2.4141	
Pglyrp1	-1.4418		1.0772	
Mmp8	-2.4735		1.2149	1.5833
S100a8	-2.9328		1.6087	1.583
Sectm1b	-1.4392			2.2915

Figure 10. Venn analysis of DEGs from different groups.

light on the potential use of this traditional Chinese medicine in MIRI management. However, more detailed mechanistic studies and clinical trials are needed to confirm these findings and to guide the safe and effective use of SKDW in clinical settings.

Conflict of Interest

The authors declare that they have no conflict of interests.

Data Availability

The datasets generated during and/or analyzed during the current study are available from the corresponding author upon reasonable request.

Informed Consent

Not applicable.

Ethics Approval

This study was carried out according to the recommendations of the U.S. NIH Guidelines for the Care and Use of Laboratory Animals. The protocol was approved by the Affiliated Hospital of Changchun University of Traditional Chinese Medicine (No.: 2021442).

ORCID ID

Jingzhou Zhang: 0009-0003-9921-3646.

Authors' Contributions

Ye Sun: conceptualization, funding acquisition, administrative support. Qiong Jia: methodology, laboratory work, validation. Lin Li: administrative support, medical insurance coordination. Yanqing Tong and Di Zou: writing-review, editing. Yinghui Liu: traditional Chinese medicine expertise, writing-review, editing. Jingzhou Zhang: conceptualization, supervision, writing-original draft, writing-review, editing.

Funding

Natural Science Foundation of Jilin Province (No. YDZ-J202201ZYTS201).

References

1) Wang J, Liu Y, Liu Y, Huang H, Roy S, Song Z, Guo B. Recent advances in nanomedicines for imaging and therapy of myocardial ischemia-reper-

fusion injury. J Control Release 2023; 353: 563-590.

2) Galeone A, Grano M, Brunetti G. Tumor Necrosis Factor Family Members and Myocardial Ischemia-Reperfusion Injury: State of the Art and Therapeutic Implications. Int J Mol Sci 2023; 24: 4606.
3) Zhao F, Jiang H, Zhang T, Chen H, Li W, Li X, Wang P, Xu H. Mechanism Repositioning Based on Integrative Pharmacology: Anti-Inflammatory Effect of Safflower in Myocardial Ischemia–Reperfusion Injury. Int J Mol Sci 2023; 24: 5313.
4) Huang Y, Li W, Su ZY, Kong ANT. The complexity of the Nrf2 pathway: beyond the antioxidant response. J Nutr Biochem 2015; 26: 1401-1413.
5) Bu W, Zhang Z, Ocansey DKW, Yu Z, Yang X, Liu Z, Wang X, Ke Y. Research on natural products from traditional Chinese medicine in the treatment of myocardial ischemia-reperfusion injury. Am J Transl Res 2022; 14: 1952.
6) Zhang J, Wider B, Shang H, Li X, Ernst E. Quality of herbal medicines: challenges and solutions. Complement Ther Med 2012; 20: 100-106.
7) Dong TTX, Cui X, Song ZH, Zhao K-J, Xi Y, Lo C, Tsim KWK. Chemical Assessment of Roots of <i>Panax Notoginseng</I> in China: Regional and Seasonal Variations in Its Active Constituents. J Agric Food Chem 2003; 51: 4617-4623.
8) Yin SJ, Luo Y, Zhao CP, Chen H, Zhong Z, Wang S, Wang Y, Zhang Q. Antithrombotic Effect and Action Mechanism of Salvia Miltiorrhiza and Panax Notoginseng Herbal Pair on the Zebrafish. Chin Med 2020; 15: 35.
9) Ahn HY, Lee HC, Kim K, Kim CS, Nho CW, Jang H, Pan C-H, Lee C, Jung SH. Hydroxycinnamic Acids in <i>Crepidiastrum Denticulatum</I> Protect Oxidative Stress-Induced Retinal Damage. J Agric Food Chem 2014; 62: 1310-1323.
10) Wang Y, Ding J, Song H, Teng Y, Fang X. VSIG4 regulates macrophages polarization and alleviates inflammation through activating PI3K/AKT and inhibiting TLR4/NF-κB pathway in myocardial ischemia-reperfusion injury rats. Physiol Int 2022; 109: 356-370.
11) Yellon DM, Hausenloy DJ. Myocardial reperfusion injury. N Engl J Med 2007; 357: 1121-1135.
12) Whelan RS, Kaplinskiy V, Kitsis RN. Cell death in the pathogenesis of heart disease: mechanisms and significance. Annu Rev Physiol 2010; 72: 19-44.
13) Toldo S, Abbate A. The NLRP3 inflammasome in acute myocardial infarction. Nat Rev Cardiol 2018; 15: 203-214.
14) Dhalla NS, Elmoselhi AB, Hata T, Makino N. Status of myocardial antioxidants in ischemia-reperfusion injury. Cardiovasc Res 2000; 47: 446-456.
15) Xing N, Long XT, Zhang HJ, Fu LD, Huang JY, Chaurembo AI, Chanda F, Xu YJ, Shu C, Lin KX. Research progress on effects of traditional Chinese medicine on myocardial ischemia-reperfusion injury: A review. Front Pharmacol 2022; 13: 1055248.
16) Ito Y, Ofengeim D, Najafov A, Das S, Saberi S, Li Y, Hitomi J, Zhu H, Chen H, Mayo L. RIPK1 mediates axonal degeneration by promoting inflammation and necroptosis in ALS. Science 2016; 353: 603-608.
17) Grenard P, Bresson-Hadni S, El Alaoui Sd, Chevallier M, Vuitton DA, Ricard-Blum S. Transglutaminase-mediated cross-linking is involved in the stabilization of extracellular matrix in human liver fibrosis. J Hepatol 2001; 35: 367-375.
18) Knight WD, Swoap SJ, Parsons AD, Overton JM. Central thyrotropin-releasing hormone infusion opposes cardiovascular and metabolic suppression during caloric restriction. Neuroendocrinology 2006; 83: 69-76.
19) Reiss Y, Proudfoot AE, Power CA, Campbell JJ, Butcher EC. CC chemokine receptor (CCR) 4 and the CCR10 ligand cutaneous T cell-attracting chemokine (CTACK) in lymphocyte trafficking to inflamed skin. J Exp Med 2001; 194: 1541-1547.